PHYSICAL REVIEW C **68**, 011601(R) (2003)

Probing the isovector transition strength of the low-lying nuclear excitations induced by inverse kinematics proton scattering

Dao T. Khoa*
Institute for Nuclear Science & Technique, VAEC, P.O. Box 5T-160, Nghia Do, Hanoi, Vietnam
(Received 22 April 2003; published 30 July 2003)

A compact approach based on the folding model is suggested for the determination of the isoscalar and isovector transition strengths of the low-lying ($\Delta S=\Delta T=0$) excitations induced by inelastic proton scattering measured with exotic beams. Our analysis of the recently measured inelastic ^{18,20}O+p scattering data at $E_{\rm lab}=30$ and 43 MeV/nucleon has given for the first time an accurate estimate of the isoscalar β_0 and isovector β_1 deformation parameters [which cannot be determined from the (p,p') data alone by standard methods] for 2_1^+ and 3_1^- excited states in ^{18,20}O. Quite strong isovector mixing was found in the 2_1^+ inelastic ^{20}O+p scattering channel, where the strength of the isovector form factor F_1 (prototype of the Lane potential) corresponds to a β_1 value almost three times larger than β_0 and a ratio of nuclear transition matrix elements, $M_n/M_p\simeq 4.2$.

DOI: 10.1103/PhysRevC.68.011601 PACS number(s): 25.40.Ep, 21.10.Re, 24.10.Eq, 24.10.Ht

Although the isospin dependence of the nucleon-nucleus optical potential, known by now as Lane potential [1], has been studied since a long time, very few attempts have been made to study the isospin dependence of the transition potential for *inelastic* scattering. The neutron and proton contributions to the structure of the low-lying nuclear excitations are known to be quite different [2], and the inelastic nuclear form factor contains, therefore, an isospin dependence which determines the degree of the *isovector* mixing in the inelastic scattering channel, which induces the excitation.

In general, the isospin-dependent potential is proportional to the product of the projectile and target isospins $(\boldsymbol{T}_p\boldsymbol{T}_t)$. For the heavy ions, this term has been shown [3] to be negligible and the scattering cross section is mainly determined by the isoscalar term. The situation is different in the nucleon-nucleus case where the optical potential can be written in terms of the isoscalar (IS) and isovector (IV) components [1] as

$$U(R)=U_0(R)\pm\varepsilon U_1(R),\ \varepsilon=(N-Z)/A, \tag{1}$$

where the plus sign pertains to incident neutron and the minus sign to incident proton. The strength of the Lane potential U_1 is known from (p,p) and (n,n) elastic scattering and (p,n) reactions studies, to be around 30–40 % of the U_0 strength. In many cases, inelastic nucleon-nucleus scattering cross section can be reasonably well described, in the distorted-wave Born approximation (DWBA) or coupled channel formalism by a collective-model prescription, where the inelastic form factor F is obtained by ''deforming'' the optical potential (1) with a scaling factor δ known as the nuclear deformation length,

$$F(R)=\delta\frac{dU(R)}{dR}=\delta_0\frac{dU_0(R)}{dR}\pm\varepsilon\delta_1\frac{dU_1(R)}{dR}. \tag{2}$$

The explicit knowledge of δ_0 and δ_1 would give us vital structure information about the IS and IV transition strengths of the excitation under study. There are only two types of experiment, which might allow one to determine δ_0 and δ_1 using prescription (2):

(i) (p,n) reaction leading to the *excited* isobar analog state. It was shown, however, that the two-step mechanism usually dominates this process and the calculated cross sections were insensitive to δ_1 values [4].

(ii) Another way is to extract $\delta_{0(1)}$ from the (p,p') and (n,n') data measured at about the same incident energy and exciting the same state of the target [4,5]. Since $\varepsilon U_1/U_0$ is only about few percent, the uncertainty of such a method can be quite large. Moreover, the most interesting data are now being measured with the secondary (unstable) beams and (given the beam intensities much weaker than those of stable beams) it is technically not feasible to perform simultaneously (p,p') and (n,n') measurements (in the inverse kinematics) with those beams.

From a theoretical point of view, the form factor (2) has been shown to have inaccurate radial shape, which tends to underestimate the transition strength, especially, for high-multipole excitations induced by inelastic heavy-ion scattering [6,7]. Since the nuclear deformation is directly linked to the ''deformed'' shape of the excited nucleus, instead of deforming the optical potential (2), we build up the proton and neutron transition densities of a 2^λ-pole excitation ($\lambda\geqslant 2$) using Bohr-Mottelson (BM) prescription [8] separately for protons and neutrons

$$\rho_\lambda^\tau(r)=-\delta_\tau\frac{d\rho_{\rm g.s.}^\tau(r)}{dr},\ \text{with}\ \ \tau=p,n. \tag{3}$$

Here $\rho_{\rm g.s.}^\tau(r)$ are the proton and neutron ground state (g.s.) densities and δ_τ are the corresponding deformation lengths. Given the explicit proton and neutron transition densities and an effective isospin-dependent nucleon-nucleon (*NN*) interaction, one obtains from the folding model [9] the inelastic proton-nucleus form factor (in terms of IS and IV parts) as

*Email address: khoa@vaec.gov.vn

$$F(R)=F_0(R)-\varepsilon F_1(R), \tag{4}$$

where $F_0(R)=V_{IS}(R)$ and $F_1(R)=-V_{IV}(R)/\varepsilon$. The explicit formulas of $V_{IS(IV)}$ are given in Ref. [9]. One can see that $F_1(R)$ is prototype of the Lane potential for inelastic scattering. In both elastic and inelastic channels, V_{IS} and V_{IV} are determined by the sum $(\rho_n+\rho_p)$ and difference $(\rho_n-\rho_p)$ of the neutron and proton densities [9], respectively. It is, therefore, natural to represent the IS and IV parts of the nuclear density as

$$\rho^{0(1)}_{\lambda(\text{g.s.})}(r)=\rho^{n}_{\lambda(\text{g.s.})}(r)\pm\rho^{p}_{\lambda(\text{g.s.})}(r). \tag{5}$$

On the other hand, one can generate using the same BM prescription the IS and IV transition densities by deforming the IS and IV parts of the nuclear g.s. density,

$$\rho^{0(1)}_{\lambda}(r)=-\delta_{0(1)}\frac{d[\rho^{n}_{\text{g.s.}}(r)\pm\rho^{p}_{\text{g.s.}}(r)]}{dr}. \tag{6}$$

The explicit expressions for the IS and IV deformation lengths are easily obtained from Eqs. (5) and (6), after some integration in parts, as

$$\delta_0=\frac{N\langle r^{\lambda-1}\rangle_n\delta_n+Z\langle r^{\lambda-1}\rangle_p\delta_p}{A\langle r^{\lambda-1}\rangle_A}, \tag{7}$$

$$\delta_1=\frac{N\langle r^{\lambda-1}\rangle_n\delta_n-Z\langle r^{\lambda-1}\rangle_p\delta_p}{N\langle r^{\lambda-1}\rangle_n-Z\langle r^{\lambda-1}\rangle_p}. \tag{8}$$

The radial momenta $\langle r^{\lambda-1}\rangle_{n,p,A}$ are taken over the neutron, proton and total g.s. densities, respectively,

$$\langle r^{\lambda-1}\rangle_x=\int_0^\infty\rho^{x}_{\text{g.s.}}(r)r^{\lambda+1}dr\Big/\int_0^\infty\rho^{x}_{\text{g.s.}}(r)r^2dr. \tag{9}$$

The transition matrix element associated with a given component of nuclear transition density is

$$M_x=\int_0^\infty\rho^{x}_{\lambda}(r)r^{\lambda+2}dr. \tag{10}$$

Realistic estimate for M_n/M_p or M_1/M_0 should give important information on the IS and IV transition strengths,

$$\frac{M_n}{M_p}=\frac{N\langle r^{\lambda-1}\rangle_n\delta_n}{Z\langle r^{\lambda-1}\rangle_p\delta_p}, \tag{11}$$

$$\frac{M_1}{M_0}=\frac{(N\langle r^{\lambda-1}\rangle_n-Z\langle r^{\lambda-1}\rangle_p)\delta_1}{(A\langle r^{\lambda-1}\rangle_A)\delta_0}. \tag{12}$$

It is useful to note that the ratios of transition matrix elements in the two representations are related by

$$M_n/M_p=(1+M_1/M_0)/(1-M_1/M_0). \tag{13}$$

If one assumes that the excitation is purely *isoscalar* and the neutron and proton densities have the same radial shape, scaled by the ratio N/Z, then $\delta_n=\delta_p=\delta_0=\delta_1$,

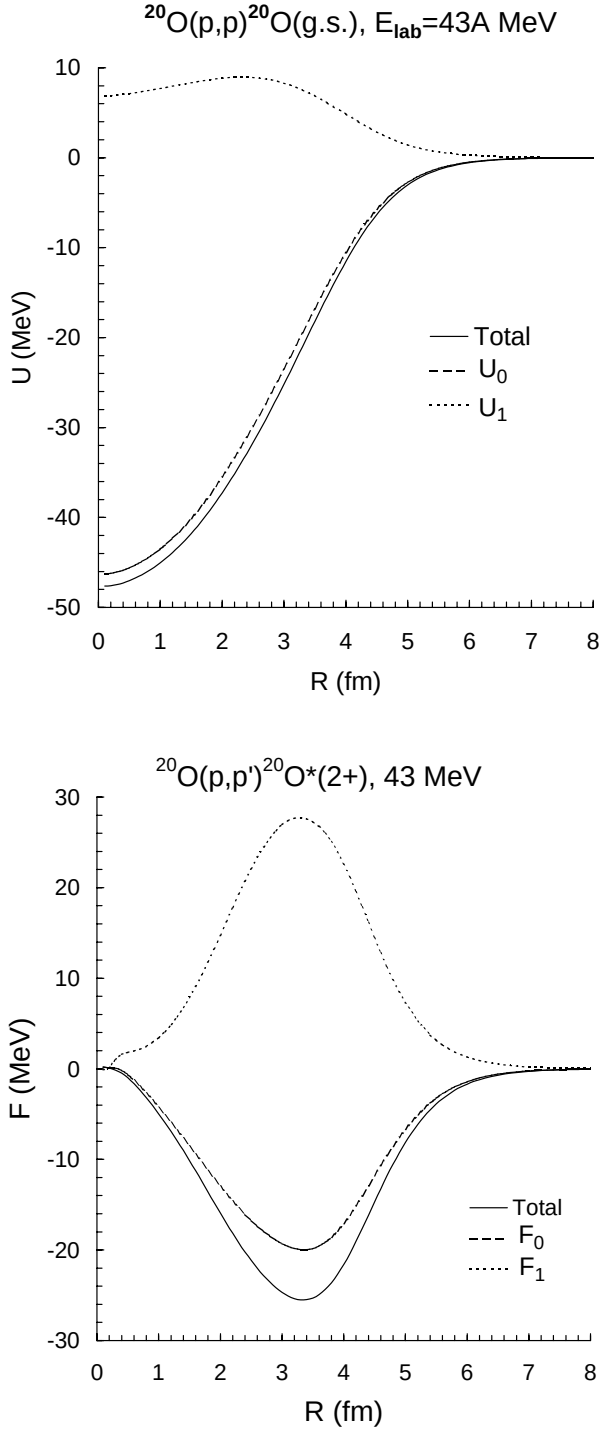

FIG. 1. Real folded optical potential (upper panel) and 2^+ inelastic form factor (lower panel) for $^{20}\text{O}+p$ system. U_1 and F_1 show strength and shape of the Lane potential in the elastic and 2^+ inelastic channels, respectively.

$$\frac{M_n}{M_p}=\frac{N}{Z}\ \text{and}\ \frac{M_1}{M_0}=\frac{N-Z}{A}=\varepsilon. \tag{14}$$

Therefore, any significant difference between M_n/M_p and N/Z (or between M_1/M_0 and ε) would directly indicate an isovector mixing effect.

TABLE I. Deformation parameters [$\beta_x = \delta_x/(1.2A^{1/3})$] and the ratios of transition matrix elements for 2_1^+ and 3_1^- states in ^{18,20}O given by our folding + DWBA analysis of inelastic ^{18,20}O+p scattering data at 30 and 43 MeV/nucleon. J_1/J_0 is the ratio of the volume integrals (per interacting nucleon pair) of F_1 and F_0 parts of the inelastic form factor (4).

				^{18}O ($N/Z=1.25, \varepsilon=0.11$)				
λ^π	β_p	β_n	M_n/M_p	β_0	β_1	M_1/M_0	J_1/J_0	Data
2^+	0.331±0.006	0.455±0.023	1.80±0.13	0.401±0.016	0.861±0.034	0.286±0.023	−0.992±0.089	[10]
3^-	0.461±0.003	0.453±0.022	1.35±0.08	0.456±0.014	0.432±0.016	0.149±0.010	−0.410±0.029	[10]
				^{20}O ($N/Z=1.50$, $\varepsilon=0.20$)				
2^+	0.250±0.009	0.653±0.032	4.25±0.28	0.500±0.020	1.295±0.052	0.619±0.050	−1.258±0.101	[10]
2^+	0.250±0.009	0.635±0.032	4.13±0.27	0.489±0.019	1.248±0.050	0.611±0.050	−1.234±0.099	[11]
3^-	0.437±0.003	0.381±0.019	1.55±0.09	0.401±0.012	0.308±0.009	0.216±0.013	−0.281±0.017	[10]

Note that if one neglects the difference between different radial momenta $\langle r^{\lambda-1}\rangle_x$, then expressions (11) and (12) are reduced to those used earlier for the "experimental" determination of M_n/M_p [2] and M_1/M_0 [5] ratios,

$$\frac{M_n}{M_p} = \frac{N}{Z}\frac{\delta_n}{\delta_p} \quad \text{and} \quad \frac{M_1}{M_0} = \frac{(N-Z)\,\delta_1}{A\,\delta_0}. \tag{15}$$

We further choose the proton deformation length δ_p so that the *measured* electric transition rate is given by $B(E\lambda\uparrow) = e^2|M_p|^2$. As a result, the only free parameter to be determined from the DWBA fit to the inelastic scattering data is the neutron deformation length δ_n if the experimental $B(E\lambda\uparrow)$ value is known (from, e.g., γ-decay strength). Other transition matrix elements and deformation parameters can be directly obtained from $\delta_{p(n)}$ using Eqs. (3)–(12). This is the main advantage of our approach compared to the standard analysis using simple prescription (2).

In the present work we have extensively analyzed the elastic and inelastic ^{18,20}O+p scattering data at 43 [10] and ^{20}O+p data at 30 MeV/nucleon [11]. The optical model (OM) analysis was done using the real folded potential [9] obtained with the density- and isospin dependent CDM3Y6 interaction [12] and microscopic g.s. densities given by the Hartree-Fock-Bogoliubov approach [13]. The imaginary optical potential was parametrized in a Woods-Saxon (WS) form using the CH89 global systematics [14]. Elastic data are well reproduced with the WS strengths slightly adjusted by OM fit (keeping the same radius and diffuseness given by CH89 systematics) and real folded potential renormalized by a factor $N_R \approx 1.08$ and 1.03 for ^{18}O and ^{20}O, respectively. The isospin dependence of the CDM3Y6 interaction was shown earlier to reproduce the empirical symmetry energy of asymmetric nuclear matter [3], and it gives also realistic estimate for the Lane potential U_1. In both cases, the ratio of the volume integrals of U_1 and U_0 parts of the real (folded) optical potential per interacting nucleon pair is $J_1/J_0 \approx -0.37$, which agrees well with the observed trend. To illustrate the radial shape of the Lane potential, we have plotted in the upper panel of Fig. 1 the folded U_1 and U_0 potentials for ^{20}O+p system. An enhancement of U_1 strength (approaching around 10 MeV) was found near the surface, which must be due to the neutrons in the outer shell. Since the best-fit N_R factors of the folded potential are quite close to unity, our result confirms the reliability of the folding model in predicting the strength and shape of the Lane potential, given a realistic choice for the effective *NN* interaction and nuclear g.s. densities.

We discuss now the IS and IV strengths of the inelastic ^{18,20}O+p form factors. Note that ^{18}O nucleus is rather well studied and inelastic ^{18}O+p data are, therefore, quite helpful in testing the present folding approach. By adjusting M_p to the experimental $B(E2\uparrow) = 45.1 \pm 2.0\, e^2$ fm^4 [15] and $B(E3\uparrow) = 1120 \pm 11\, e^2$ fm^6 [16] for the first 2^+ and 3^- states in ^{18}O, we obtain $\delta_p = 1.040 \pm 0.020$ and 1.449 ± 0.008 fm, respectively. The $E2$ transition strength is more fragmented in ^{20}O and the experimental $B(E2\uparrow) = 28.1 \pm 2.0\, e^2$ fm^4 [15] for 2_1^+ state. There are no $B(E3\uparrow)$ data available for 3_1^- state in ^{20}O, and we have assumed a value $B(E3\uparrow) = 1200 \pm 12\, e^2$ fm^6, which was estimated from the experimental $B(E3\uparrow)$ for 3_1^- state in ^{18}O using the ratio of the $B(E3\uparrow)$ values calculated for these two cases in the quasiparticle random phase approximation (QRPA) [10]. As a result, we obtain the proton deformation lengths $\delta_p = 0.815 \pm 0.029$ and 1.424 ± 0.008 fm for 2_1^+ and 3_1^- states in ^{20}O, respectively. Note that the numerical uncertainties of the obtained proton deformation lengths are fully determined by those of the measured $B(E\lambda\uparrow)$ values. Using the best-fit neutron deformation length from the DWBA analysis of the inelastic data under consideration, realistic shape of the Lane potential in an inelastic scattering channel can be obtained. As an example, we have plotted in the lower panel of Fig. 1 the 2^+ inelastic form factor for ^{20}O+p system, where contributions by the IS and IV components are shown explicitly. We further assign a numerical uncertainty of around 5% to the deduced neutron deformation length, which gives a cross-section shift within the experimental errors. The numerical uncertainties of all the deformation parameters and ratios of transition matrix elements given in Table I were deduced directly from those found for the proton and neutron deformation lengths.

Since the CDM3Y6 interaction is *real*, only real nuclear, Coulomb and spin-orbit transition form factors for ^{18,20}O are obtained from the folding calculation [9]. The imaginary nuclear form factor is obtained by deforming the imaginary part of the optical potential with δ_0, which is iteratively found from the DWBA fit to the data. Fortunately, nucleon

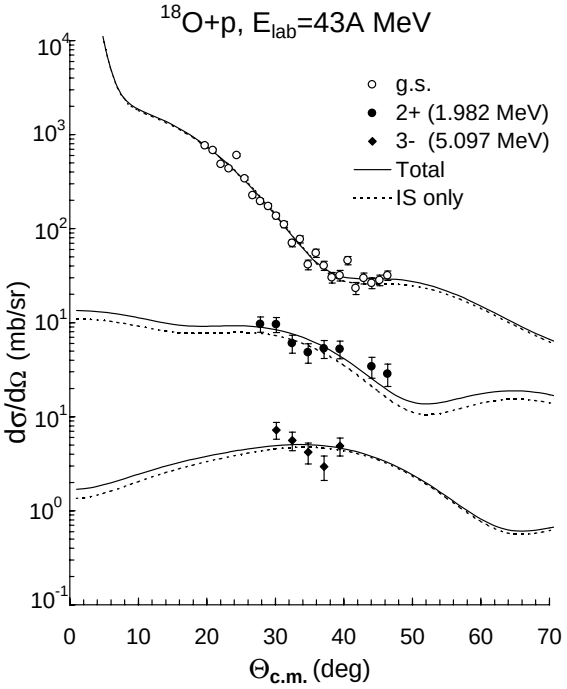

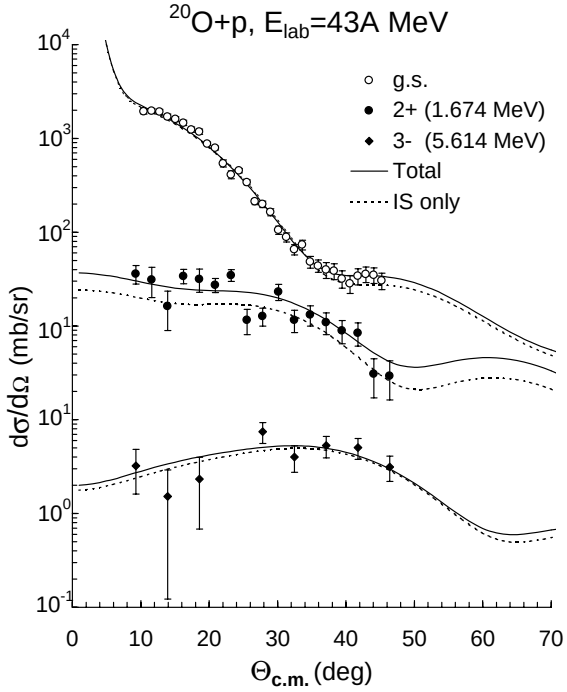

FIG. 2. Elastic and inelastic ^{18,20}O+p scattering data at 43 MeV/nucleon in comparison with DWBA cross sections given by the folded form factors. Cross sections given by the isoscalar potentials alone are plotted as dotted curves.

inelastic scattering at low-to-medium energies is not dominated by the imaginary coupling [17], and the DWBA cross section is strongly sensitive to the real form factor, which allows an accurate deduction of the (neutron) deformation length.

Elastic and inelastic ^{18,20}O+p cross sections (at 43 MeV/nucleon) obtained with the best-fit deformation parameters

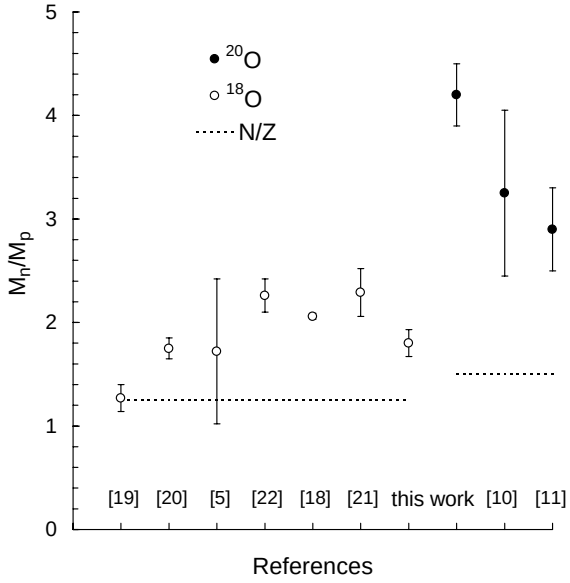

FIG. 3. M_n/M_p ratios extracted for the lowest 2^+ excitations in ^{18,20}O isotopes.

are plotted in Fig. 2. One can see that the IV contribution is small in the elastic and 3^- inelastic channels. We found that 3_1^- state is dominantly isoscalar, with the best-fit M_n/M_p ratio slightly above N/Z and M_1/M_0 ratio close to ε (see Table I). This result is well expected because the 3_1^- states in ^{18,20}O isotopes were shown by the QRPA calculation [10] to consist mainly of the $(1p_{1/2}^{-1},1d_{5/2})$ proton configuration. Strong IV effect was found in 2_1^+ inelastic channel. Structure of 2_1^+ state in ^{18}O has been investigated in numerous studies, such as (p,p') reactions, at low [5] and intermediate energies [18] or (π,π') reactions [19–21], and the weighted average of those results [11] gives $M_n/M_p \approx 2$. This value also agrees fairly with that deduced from a pure isospin-symmetry assumption that M_p obtained for the mirror ^{18}Ne nucleus would yield M_n for the corresponding excited state in ^{18}O [22]. M_n/M_p ratios deduced from these studies are compared with our result in Fig. 3.

One can see that our result is in a satisfactory agreement with the empirical data. The obtained IV deformation ($\beta_1 \approx 0.86$) is about twice the IS deformation, which indicates a significant IV mixing in this case. Prior to our work, the only attempt to deduce β_1 for 2_1^+ state in ^{18}O that we could find in the literature is the DWBA analysis of (p,p') and (n,n') scattering data at 24 MeV [5], which gives $\beta_0 \approx 0.4$ and $\beta_1 \approx 1.0 \pm 0.5$, using prescription (2) and assuming β_0 to be the average of the β values obtained with (p,p') and (n,n') data. Although the uncertainty associated with β_1 is large, this result agrees reasonably with $\beta_{0(1)}$ given by our analysis.

In contrast to the ^{18}O case, the (p,p') excitation of 2_1^+ state in radioactive ^{20}O nucleus has been studied only recently in the inverse kinematics proton scattering measurements at 43 [10] and 30 MeV/nucleon [11]. A simple folding analysis using the microscopic QRPA transition densities and JLM interaction [10] has failed to fit the data at 43 MeV.

Khan *et al.* obtained $M_n/M_p \approx 1.10 \pm 0.24$ and 3.25 ± 0.80 for 2_1^+ excitation in ^{18}O and ^{20}O, respectively, after renormalizing the QRPA densities to the best DWBA fit to the data [10]. If one uses a simple (probe-dependent) collective model in the analysis of (p,p') data [11] measured at 24 and 30 MeV for ^{18}O and ^{20}O, these values become $M_n/M_p \approx 1.50 \pm 0.17$ and 2.9 ± 0.4, respectively. Despite the uncertainty of these data, they do indicate a strong IV mixing in the 2_1^+ excitation in ^{20}O. Our result shows even stronger IV transition strength for this state and M_n/M_p ratio obtained with the best-fit neutron deformation length from our folding analysis of 43-MeV [10] and 30-MeV data [11] is around 4.25 and 4.13, respectively. We adopted, therefore, an average value of $M_n/M_p \approx 4.2 \pm 0.3$ from the values obtained in these two cases. The IV deformation, given for the first time for 2_1^+ state in ^{20}O ($\beta_1 \approx 1.3$), is nearly three times the IS deformation ($\beta_0 \approx 0.5$), and $M_1/M_0 \approx 0.6 = 3\varepsilon$. This leads to a ratio of the volume integrals of F_1 and F_0 folded form factors $J_1/J_0 \approx -1.25$, which is significantly higher than that found in the elastic channel. The relative IV strength in the inelastic 2_1^+ channel is, therefore, $\varepsilon|J_1/J_0| \approx 25\%$, with the IV form factor peaked at the surface (see Fig. 1). This significant contribution by the Lane potential in the 2_1^+ inelastic channel of $^{20}O+p$ system amounts up to 40–50% of the total cross section over the whole angular range as shown in Fig. 2.

In conclusion, a compact folding approach is developed for a consistent study of strength and shape of the Lane potential in both elastic and inelastic proton-nucleus scattering, and to deduce from the analysis of (p,p') data the IS and IV deformation parameters which, otherwise, can be deduced only if there are (p,p') and (n,n') data available at the same energy for the same target. With more data being measured with the unstable beams, our model should be helpful for the determination of the isospin distribution in the low-lying excited states of exotic nuclei, which can be used as important ''database'' for further nuclear structure studies. The use of microscopic nuclear densities in our approach should be encouraged to test the nuclear structure model ingredients by studying the known excitations and, consequently, to predict the isospin character of those not yet measured.

The author thanks Paul Cottle, Marcella Grasso, Elias Khan, and Kirby Kemper for very helpful correspondence. The research was supported, in part, by the Natural Science Council of Vietnam.

[1] A.M. Lane, Phys. Rev. Lett. **8**, 171 (1962).
[2] A.M. Bernstein, V.R. Brown, and V.A. Madsen, Comments Nucl. Part. Phys. **11**, 203 (1983).
[3] Dao T. Khoa, W. von Oertzen, and A.A. Ogloblin, Nucl. Phys. **A602**, 98 (1996).
[4] R.W. Finlay, J. Rapaport, V.R. Brown, V.A. Madsen, and J.R. Comfort, Phys. Lett. **84B**, 169 (1979).
[5] P. Grabmayr, J. Rapaport, and R.W. Finlay, Nucl. Phys. **A350**, 167 (1980).
[6] J.R. Beene, D.J. Horen, and G.R. Satchler, Phys. Lett. B **344**, 67 (1995); Nucl. Phys. **A596**, 137 (1996).
[7] Dao T. Khoa and G.R. Satchler, Nucl. Phys. **A668**, 3 (2000).
[8] A. Bohr and B. R. Mottelson, *Nuclear Structure* (Benjamin, New York, 1975), Vol. 2.
[9] Dao T. Khoa, E. Khan, G. Colò, and N. Van Giai, Nucl. Phys. **A706**, 61 (2002).
[10] E. Khan *et al.*, Phys. Lett. B **490**, 45 (2000).
[11] J.K. Jewell *et al.*, Phys. Lett. B **454**, 181 (1999).
[12] Dao T. Khoa, G.R. Satchler, and W. von Oertzen, Phys. Rev. C **56**, 954 (1997).
[13] M. Grasso, N. Sandulescu, N. Van Giai, and R.J. Liotta, Phys. Rev. C **64**, 064321 (2001).
[14] R.L. Varner, W.J. Thompson, T.L. McAbee, E.J. Ludwig, and T.B. Clegg, Phys. Rep. **201**, 57 (1991).
[15] S. Raman, C.W. Nestor, Jr., and P. Tikkanen, At. Data Nucl. Data Tables **78**, 1 (2001).
[16] R.H. Spear, At. Data Nucl. Data Tables **42**, 55 (1989).
[17] G. R. Satchler, *Direct Nuclear Reactions* (Clarendon, Oxford, 1983).
[18] J. Kelly *et al.*, Phys. Lett. **169B**, 157 (1986).
[19] J. Jansen *et al.*, Phys. Lett. **77B**, 359 (1978).
[20] S. Iversen *et al.*, Phys. Rev. Lett. **40**, 17 (1978); Phys. Lett. **82B**, 51 (1979).
[21] S.J. Seestrom-Morris, D. Dehnhard, M.A. Franey, D.B. Holtkamp, C.L. Blilie, C.L. Morris, J.D. Zumbro, and H.T. Fortune, Phys. Rev. C **37**, 2057 (1988).
[22] A.M. Bernstein, V.R. Brown, and V.A. Madsen, Phys. Rev. Lett. **42**, 425 (1979).